

## Fracton dynamics of percolating elastic networks: Energy spectrum and localized nature

K. Yakubo and T. Nakayama

*Department of Applied Physics, Hokkaido University, Sapporo 060, Japan*

(Received 16 January 1989)

We have performed computer experiments on the dynamics of two- and three-dimensional (2D and 3D) percolating elastic networks with the site number  $N > 10^5$ . The densities of vibrational states (DOS's) for these large percolating networks as well as the mode patterns of fractons are obtained. It is confirmed, for both 2D and 3D networks, that the DOS is proportional to  $\omega^{\bar{d}-1}$  with  $\bar{d}$  close to  $\frac{4}{3}$  in the regime above the characteristic frequency  $\omega_c$ . We could not find the notable steepness or hump in the DOS at the vicinity of a phonon-fracton crossover frequency  $\omega_c$ , i.e., our results were incompatible with the prediction by the effective-medium theory. Specific realizations of mode patterns show that the core of fracton excitations falls off sharply at their edges, and that the localized nature is quite unique.

### I. INTRODUCTION

Percolating networks have a fractal geometry on smaller length scales than the percolation correlation length  $\xi_p$ . This behavior crosses over to the Euclidean geometry on larger scales than  $\xi_p$ . The density of vibrational states (DOS) with wavelengths much larger than  $\xi_p$  should obey the conventional Debye law,  $D(\omega) \sim \omega^{d-1}$ , where  $d$  is the Euclidean dimension. These excitations are called *phonons*.

The scaling argument has suggested that the DOS for fractal networks follows the universal law,<sup>1,2</sup>

$$D(\omega) \sim \omega^{\bar{d}-1}, \quad (1.1)$$

where  $\bar{d}$  is the fracton dimensionality.<sup>1,2</sup> When percolating networks are characterized by the fractal dimension  $D$  and the exponent of diffusion  $\theta$ ,  $\bar{d}$  can be expressed as  $\bar{d} = 2D/(2+\theta)$ . Alexander and Orbach<sup>1</sup> have conjectured that the fracton dimensionality  $\bar{d}$  for a percolating network is  $\frac{4}{3}$ , which is independent of the Euclidean dimension  $d$ . These excitations were named "fractons."<sup>1,3,4</sup>

Fracton excitations play an essential role in many stages of physics for topologically disordered systems. Examples are the thermal conductivity of glasses,<sup>5,6</sup> electronic relaxation with fracton emission,<sup>7</sup> Raman<sup>8-10</sup> or Brillouin<sup>11,12</sup> scattering for topologically disordered materials, spin-wave excitations on randomly diluted antiferromagnets,<sup>13,14</sup> dc conductivity due to the variable range hopping,<sup>15</sup> and ultrasonic attenuation in porous media.<sup>16</sup> None of these phenomena can be completely understood without detailed knowledge of the DOS, the dispersion relation, and the shape of the fracton wave function. Another important feature of fractons is the localized nature. It appears to have been generally accepted that fractons possess the unusual localized character called "superlocalization."<sup>17-19</sup> However, the understanding of fracton excitations (eigenmodes) is not satisfactory either theoretically or experimentally at the present stage.

Computer simulations permit one, in principle, to investigate the dynamics of percolating networks that may

be inaccessible to direct experimental study. Although computer simulations have had difficulty in treating *large* systems, which would provide a model that can be compared with laboratory experiments, the situation is changing because array-processing supercomputers have become available.

In this article, we have performed computer experiments on the dynamics of two- and three-dimensional (2D and 3D) site-percolating elastic networks. Our systems treated have the site number as *large* as  $N > 10^5$ , for which a novel numerical method developed by Williams and Maris<sup>20</sup> is employed. The DOS's for these large percolating networks as well as the mode patterns of fractons are obtained. From these mode patterns, we have found evidence of specific character of localized fractons.

In Sec. II, the model and the numerical method used in this work is described. The results of the DOS's calculations for 2D and 3D percolating networks are given in Sec. III. This section also presents numerical evidence for the localization of a fracton wave function on 2D percolating networks. Conclusions are given in Sec. IV. This paper would provide useful details for our related brief reports of Refs. 21-23.

### II. THE SITE-PERCOLATING NETWORK AND OUR NUMERICAL ALGORITHM

We consider a site-percolating network consisting of  $N$  atoms with unit mass and linear springs connecting two nearest-neighbor atoms. The equations of motion of this system are simple, as expressed by

$$\ddot{u}_i(t) + \sum_j K_{ij} u_j(t) = 0, \quad (2.1)$$

where  $u_i$  is the scalar displacement of the atom on the  $i$ th site. The force constant is taken to be  $K_{ij} = 0$  ( $i \neq j$ ) if either sites  $i$  or  $j$  are unoccupied, and  $K_{ij} = 1$  otherwise. Diagonal elements satisfy the relation  $K_{ii} = -z_i$  where  $z_i$  is the coordination number of the site  $i$ . It should be noted here, if we put  $K_{ii} = 0$ , that our system is transferred to the quantum percolation problem. The displacement  $u_i$

is assumed to have only one component. This simplification enables us to extract the intrinsic features of the dynamics of percolating systems.

In standard numerical methods, the dynamical matrix  $[K_{ij}]$  is diagonalized directly to obtain the eigenfrequencies and eigenmodes of the system described by Eq. (2.1). These methods, however, require a large amount of computer memory space (order of  $N^2$ ) and relatively long CPU time. Because of these conditions, the site number we can treat is limited in general to a few thousands. In addition, these standard numerical routines yield poor accuracy for the low-frequency eigenvalues. The method employed in the present work, introduced by Williams and Maris,<sup>20</sup> enables us to treat the eigenvalue problem of very large systems as large as  $N > 10^5$ , because the algorithm requires less memory space (order of  $N$ ) and is extraordinarily suitable for array-processing supercomputers. The method is based on the physical analogy that the eigenfrequency of the system satisfies the resonance condition when applying the periodic external force with frequency  $\Omega$  to the system.

#### A. The algorithm (Ref. 20)

The initial set at  $t=0$  is prepared in which all atoms are at rest and have zero displacements. A random force is applied to each atom at rest, which is given by

$$F_i = F_0 \cos(\phi_i) \cos(\Omega t), \quad (2.2)$$

where  $F_0$  is a constant amplitude, the phase  $\phi_i$  and  $\Omega$  are a random variable with respect to the site number  $i$  and a frequency of the external force, respectively. The averaged total energy of the system after time  $T$  becomes

$$\langle E(\Omega, T) \rangle = \frac{F_0}{4} \sum_{\lambda} \frac{\sin^2[(\omega_{\lambda} - \Omega)T/2]}{(\omega_{\lambda} - \Omega)^2}, \quad (2.3)$$

where  $\omega_{\lambda}$  is an eigenfrequency of mode  $\lambda$ . If one chooses the time interval  $T$  so that: (i) the resonance width  $\Delta\Omega$  is small enough compared with  $\Omega$ ; (ii) the number of modes in  $\Delta\Omega$  is much larger than unity, one can approximate the summand in Eq. (2.3) by the  $\delta$  function. As a result, one has the DOS of the system as

$$D(\Omega) = \frac{8\langle E(\Omega, T) \rangle}{\pi T F_0^2 N}. \quad (2.4)$$

In order to obtain the DOS, our task is to compute the averaged total energy  $\langle E(\Omega, T) \rangle$ .

The mode patterns can be obtained by the following procedures. If a certain periodic external force  $F_i$  acts on each atom at rest, the amplitudes of several eigenmodes belonging to frequencies close to  $\Omega$  are enhanced during the appropriate time interval  $\tilde{T}$ . These amplitudes are written as

$$u_i^{(1)} = \sum_{\lambda, j} F_j e_i(\lambda) e_j(\lambda) h(\Omega, \omega_{\lambda}, \tilde{T}), \quad (2.5)$$

where

$$h(\Omega, \omega_{\lambda}, \tilde{T}) = \frac{2\sin[(\omega_{\lambda} - \Omega)\tilde{T}/2]\sin[(\omega_{\lambda} + \Omega)\tilde{T}/2]}{\Omega^2 - \omega_{\lambda}^2},$$

and  $e_i(\lambda)$  is the displacement pattern of a normal mode  $\lambda$ . As a next step, the amplitude of the external force applied to an atom is replaced by

$$F_i^{(1)} = u_i^{(1)}.$$

The system is driven, starting again with all atoms at rest, for a time interval  $\tilde{T}$  under the new external force  $F_i^{(1)}$ . Repeating this procedure  $p$  times, the displacement of atom  $i$  becomes

$$u_i^{(p)} = \sum_{\lambda, j} F_j e_i(\lambda) e_j(\lambda) h^p(\Omega, \omega_{\lambda}, \tilde{T}). \quad (2.6)$$

Thus, for sufficiently large  $p$ , only the eigenmode belonging to the eigenfrequency closest to the frequency  $\Omega$  of the external force can survive and all other remaining modes vanish.

This algorithm requires a memory space of order  $N$ . Since the total energy  $\langle E \rangle$  involves less statistical fluctuation as the system becomes large, the approximation for deriving Eq. (2.4) becomes more accurate for larger  $N$ . To summarize, this method has the following advantages: (i) One can apply this algorithm to a very large system ( $N > 10^5$ ); (ii) It is possible to calculate quite accurately the DOS in the low-frequency regime; (iii) The eigenmode (mode pattern) belonging to a given eigenfrequency can be arbitrarily selected; (iv) The algorithm is very suitable to vectorize the computer program when utilizing an array-processing supercomputer. In particular, the first advantage (i) is crucial for our purpose for two reasons: one can avoid both the boundary effects and the sample dependence on vibrational excitations, i.e., all features of randomness of the system are involved in one percolating sheet.

#### B. The ensemble-averaged shape of localized excitations

At first, we have to determine the *spatial center* of the fracton eigenmode from a smoothly leveled mode pattern. The smoothly leveled mode-pattern was formed by the following way. The absolute value of the time-averaged mode pattern  $\{\bar{u}_i\}$  is calculated from the relation,

$$\bar{u}_i = \int_0^T |u_i(t)| dt / T, \quad (2.7)$$

where  $\omega T \gg 1$ . This mode pattern  $\{\bar{u}_i\}$  is still bumpy. Therefore, the time-averaged amplitude of the  $i$ th site is changed to the value averaged over the amplitudes of nearest-neighbor sites of the  $i$ th site and the  $i$ th site itself. For example, for the site  $i$  with coordination number  $z$ , a newly evaluated amplitude is written as

$$\bar{u}_i^{(1)} = \frac{1}{z+1} \left[ \bar{u}_i + \sum_{j \in N_i} \bar{u}_j \right],$$

where  $N_i$  is a set of nearest neighbors of the  $i$ th site and  $\bar{u}_i$  is zero if the  $i$ th site is unoccupied. The first leveled mode pattern  $\{\bar{u}_i^{(1)}\}$  becomes smooth compared with  $\{\bar{u}_i\}$ . The second leveled mode pattern  $\{\bar{u}_i^{(2)}\}$  is calculated from the pattern  $\{\bar{u}_i^{(1)}\}$  in the same way. Repeating this procedure an appropriate number of times  $m$ , the  $m$ th leveled mode pattern  $\{\bar{u}_i^{(m)}\}$  is calculated from

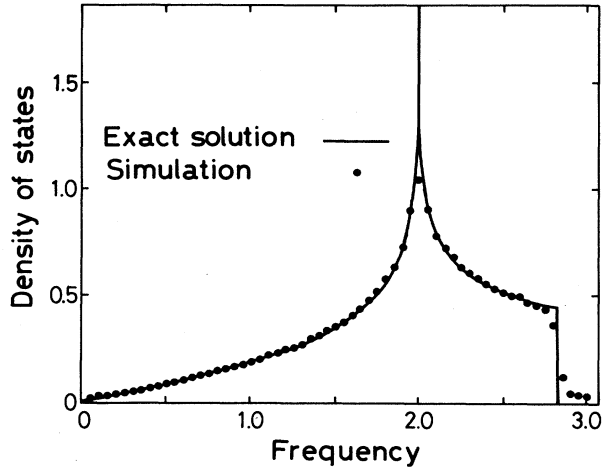


FIG. 1. The DOS for a square lattice per one atom. The angular frequency  $\omega$  is obtained in units of mass of particles  $m = 1$  and force constant  $K = 1$ . The solid line shows the exact solution for the infinite system. Filled circles are our experimental results for a  $100 \times 100$  square lattice.

$$\bar{u}_i^{(m)} = \frac{1}{z+1} \left[ \bar{u}_i^{(m-1)} + \sum_{j \in N_i} \bar{u}_j^{(m-1)} \right]. \quad (2.8)$$

This set of the amplitudes  $\bar{u}_i^{(m)}$  has a unique *maximal* point. This position at  $R_0$  is identified with the *center* of the localized fracton excitation. In our case of percolating networks formed on  $700 \times 700$  square lattices, the repeating times  $m$  were around 100.

Next, we must compute the ensemble-averaged shape of fracton wave functions from the time-averaged mode patterns  $\{\bar{u}_i\}$  of Eq. (2.7) at a distance  $r$  from the center  $R_0$ . To take the ensemble average from as many fractons as possible, several fractons are retained consciously on

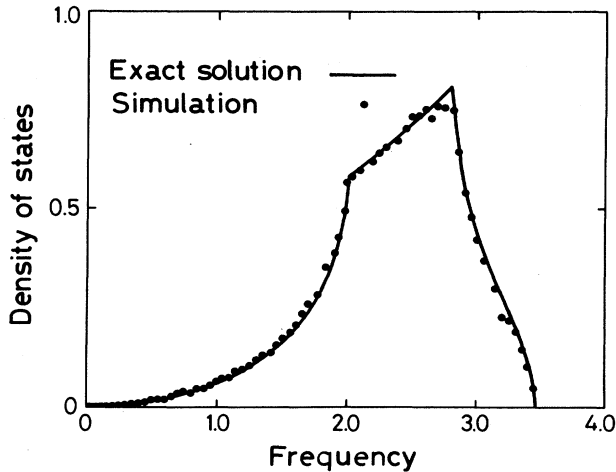


FIG. 2. The DOS for a simple cubic lattice per one atom. The solid line indicates the exact solution for the infinite system. Filled circles are our results on a  $30 \times 30 \times 30$  simple cubic lattice.

one percolating network for efficient computation. In fact, we can choose the appropriate times  $p$  in Eq. (2.6) so that several fractons can survive on a network. It is, however, necessary that these modes are enough apart from each other. We have averaged over the order of 100 fracton modes in order to obtain the precise shape of the ensemble-averaged fracton.

### C. The accuracy of our procedure

We have checked the accuracy of the above techniques. As a first step, the DOS's on a square and cubic lattice have been calculated by our routine. The exact solution for the DOS's for scalar displacement on a infinite square and cubic lattice were given by Montrol and Potts.<sup>24</sup> These exact DOS's are shown by solid lines in Figs. 1 and 2. Our numerical results are indicated by filled circles. Figure 1 shows the result for a  $100 \times 100$  square lattice and the result for a  $30 \times 30 \times 30$  cubic lattice is given in

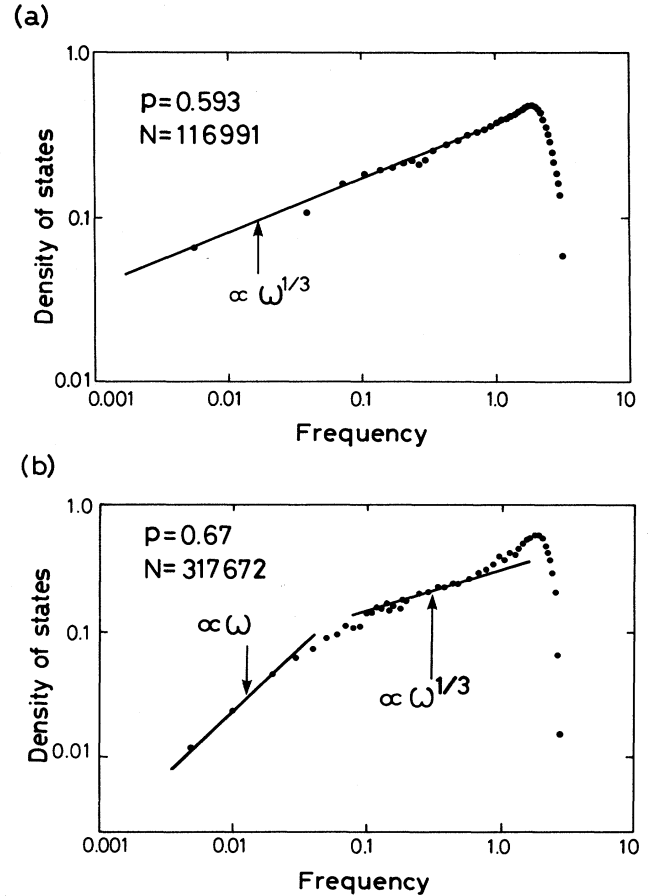


FIG. 3. The DOS's for 2D site-percolating networks at two different percolation concentrations. Filled circles indicate our numerical results and the straight lines are only a guide to the eye. (a) The DOS per site at the percolation threshold  $p_c$  ( $=0.593$ ). The network is formed on a  $700 \times 700$  square lattice and contains 116,991 atoms. (b) The DOS per site at  $p=0.67$  formed on a  $700 \times 700$  square lattice. The network size is 317 672.

Fig. 2. Both of them agree well with the exact solutions; especially the agreement in the very-low-frequency regime is excellent. The DOS's near the cutoff frequency  $\omega_D$  deviate slightly from the exact solution. This comes from the effect of the finite width of the resonance peak described by Eq. (2.3).

We have examined our routine of computing the shape of the localized wave function by comparing the localized mode pattern on a linear chain calculated by our method with that of the corresponding exact solution obtained by Montrol and Potts.<sup>24</sup> The system was constructed of 99 atoms with unit mass, and one light impurity with mass  $m=0.8$  located in the center of the linear chain, which are connected by linear springs (force constant  $K=1$ ). The exact solution for the wave function of localized impurity state is written as

$$|\phi(r,t)| = \phi_0 \exp[-r \ln|b| + i\omega t], \quad (2.9)$$

where

$$b = -\frac{2\omega_p}{\omega_D^2} [\omega_p - (\omega_p^2 - \omega_D^2)^{1/2}] + 1.$$

Here,  $r$  denotes the distance from the impurity site, and  $\omega_D$  is the Debye's cutoff frequency ( $\omega_D=2$  for 1D chain). The eigenfrequency of the localized impurity state  $\omega_p$  is determined by mass ratio  $\gamma$  (in our case,  $\gamma=0.8$ ) as expressed by

$$\omega_p^2 = \frac{\omega_D^2}{\gamma(2-\gamma)}. \quad (2.10)$$

As seen by Eq. (2.10), the light-mass impurity state should have the eigenfrequency  $\omega_p=2.041$  and the time-averaged wave function takes the form

$$\phi \sim \exp[-(r/d)^a],$$

where  $d = -1/\ln|b| = 2.466$  and  $a=1$ . Our numerical result provides  $a=1.005$  and  $d=2.506$  by setting the parameter  $p=5$  in Eq. (2.6) and choosing  $\bar{T}$  as  $\bar{T}\omega_D=800$ .

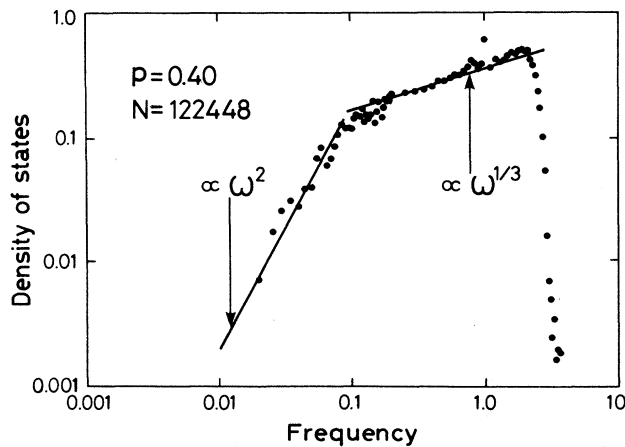


FIG. 4. The DOS per site for a 3D site-percolating network at  $p=0.4$  formed on a  $70 \times 70 \times 70$  simple cubic lattice. The network size is  $N=122448$ .

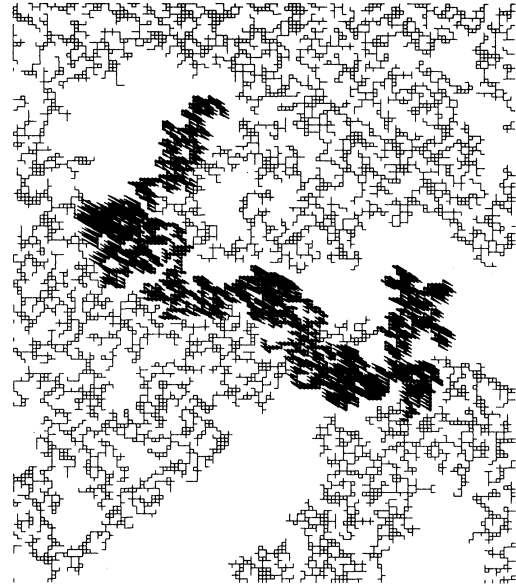


FIG. 5. Magnified figure of vibrational mode with angular frequency  $\omega=0.02$  excited on a network at the percolation threshold  $p_c=0.593$ . The network is formed on a  $70 \times 70$  square lattice and the size is 169 576. The displacements of atoms are shown by oblique arrows. Note that arrows for very small amplitudes are omitted in this figure.

The agreement between our numerical result and the exact solution can be improved by increasing the site number.

### III. RESULTS OF COMPUTER EXPERIMENTS

#### A. Densities of states for 2D and 3D percolating networks

We have computed the DOS's for 2D and 3D percolating networks. Our results of the DOS for 2D percolating networks are shown in Fig. 3 by filled circles. Figure 3(a) shows the DOS at the percolation threshold  $p_c (=0.593)$ .

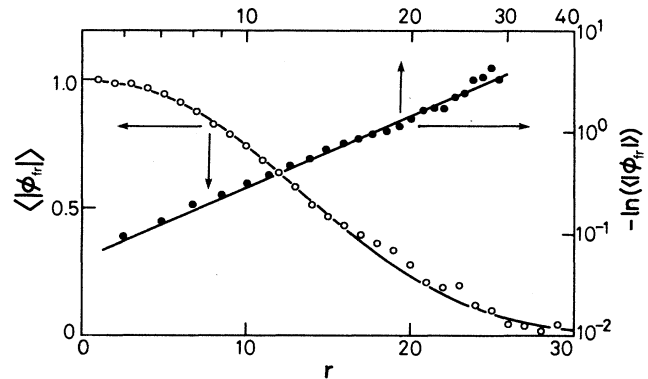


FIG. 6. The ensemble-averaged shape of the core of fractons as a function of a radial distance  $r$  (open circles) in unit of atomic spacing  $a=1$ , and the log-log plot of  $r$  and  $-\ln\langle |\phi_r| \rangle$  (filled circles). The straight line through filled circles is drawn by the least-squares fitting, and the solid line through open circles represents the same line in a linear scale. This line indicates the exponent to be  $d_\phi=2.3$  as well as  $\Lambda(\omega=0.01)=17.2$ .

This network, formed on a  $700 \times 700$  square lattice, has 116 991 atoms. The DOS was obtained under the condition that  $\omega T = 10$  and  $\omega \Delta T = 0.05$  for each frequency  $\omega$ , where  $T$  is the time defined in Eq. (2.3) and  $\Delta T$  is the time step used when solving the equation of motion of forced vibration. The solid line through filled circles with a slope of  $\frac{1}{3}$  is not from the least-squares fitting, but only a guide to the eye. This result indicates that the Alexander-Orbach conjecture,<sup>1</sup> that the DOS is proportional to  $\omega^{\bar{d}-1}$  with  $\bar{d} = \frac{4}{3}$ , is correct for 2D percolating networks with scalar displacements. It should be emphasized that this  $\omega^{1/3}$  law holds even in the low-frequency region, because the correlation length  $\xi_p$  diverges at  $p = p_c$  and the network has a fractal structure even for longer length scales. We see that the DOS does not follow the  $\omega^{1/3}$  dependence above  $\omega \sim 1$ . This is due to the fact that the system is not fractal on a length scale shorter than the wavelength corresponding to  $\omega \sim 1$ .

The DOS at  $p = 0.67$  is shown in Fig. 3(b) for the cluster size of  $N = 317\,672$ . Our result clearly indicates that the frequency dependence of the DOS is characterized into two regimes. In the higher frequency region,  $\omega_c \ll \omega \ll 1$ , the DOS is proportional to  $\omega^{1/3}$ , so that the excitations in this region are fractons. For lower frequencies ( $\omega \ll \omega_c$ ), the DOS obeys the conventional Debye's law  $D(\omega) \sim \omega$  for the 2D lattice. The crossover frequency  $\omega_c$  is close to 0.1. Note here that the wavelength corresponding to  $\omega_c$  is related to the percolation correlation length  $\xi_p$  varied as  $|p - p_c|^{-\nu}$ , where the critical exponent  $\nu$  is a positive constant. The system can be regarded as a homogeneous continuum on larger scales than  $\xi_p$ , so our numerical result in the low-frequency regime is reasonable. Figure 3(b) tells us that the DOS is smoothly connected from the phonon regime to the fracton regime. Especially, in contrast to the prediction of the effective-medium theory<sup>25-27</sup> or the numerical work by Grest and Webman,<sup>28</sup> our result does not exhibit a notable steepness or a presence of the hump in the vicinity of  $\omega_c$ .

The absence of the hump in the crossover region has been confirmed also in the case of 3D percolating networks. The DOS of a site-percolating network at  $p = 0.4$  ( $p_c = 0.312$ ) formed on a  $70 \times 70 \times 70$  simple cubic lattice is shown in Fig. 4. The network size is  $N = 122\,448$ . We can see that the DOS in the frequency region  $0.1 < \omega < 1$  is proportional to  $\omega^{1/3}$  as well as in the 2D case, that is, the Alexander-Orbach conjecture holds for the 3D case. The DOS in the low-frequency regime ( $\omega \ll 0.1$ ) obeys the Debye's law  $D(\omega) \sim \omega^2$  where the phonon-fracton

crossover frequency  $\omega_c$  is close to 0.1. It is clear that no steepness or hump of the DOS exists in the crossover region in the vicinity of  $\omega_c$ . We can find in Fig. 4 a sharp peak at  $\omega = 1$ . This peak is attributed to a vibrational mode of a single site connected by a single bond to a relatively rigid block. We have checked that such a peak in the DOS does not appear in the case of  $m = 2$  "bootstrap" percolation<sup>29,30</sup> in which there exists no site connected by a single bond.

## B. Mode patterns of fractons

The mode patterns of fractons were calculated by applying our method mentioned in the preceding section. The network at  $p_c = 0.593$  was formed on a  $700 \times 700$  square lattice and had the size 169 576.

On percolating networks at  $p_c$  all excited modes ( $\omega < 1$ ) should behave as fractons. The typical mode pattern with  $\omega = 0.02$  is shown in Fig. 5, where the displacements of atoms are shown by oblique arrows. Figure 5 shows the magnified picture of the mode pattern ( $4.4 \times 5$  times from the original  $700 \times 700$  lattice) excited on a percolating networks at  $p_c$ . We have obtained this result by choosing  $p = 16$  and  $\omega \bar{T} = 80$  in Eq. (2.6), respectively. The vibrational excitation in Fig. 5 is evidently very sharply localized at the edge. Especially, we should note that displacements of atoms in a "peninsula" (weakly connected portions in the percolating network) move in phase, and the vibrational amplitudes fall off sharply at their edges. In addition, it is interesting to note that the tail (the portion spread from the center of the figure to the lower right direction) from the core of a fracton (upper left) extends over a large distance with alternating phases (phases are indicated by directions of oblique arrows). This is because the overall center of mass of the

TABLE I. The values of localization length ( $\Lambda$ ) in a unit of atomic spacing  $a = 1$  and the geometrical exponent ( $d_\phi$ ) for various eigenfrequencies ( $\omega$ ).

$\omega$	$\Lambda$	$d_\phi$
0.005	28.13	2.25
0.006	24.18	2.24
0.007	23.49	2.34
0.008	19.41	2.26
0.010	17.20	2.31

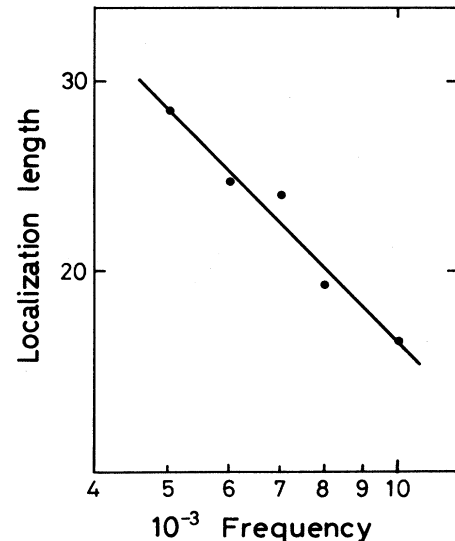


FIG. 7. Localization lengths vs frequencies of fractons plotted in a log-log scale. The straight line through filled circles is drawn by the least-squares fitting.

fracton must not move in its vibration, and there must be compensating mass outside of the core which moves in an opposite direction. Indeed, we have the relation  $\sum_i u_i = 0$  (this implies that a fracton is orthogonal to a uniform translation).

### C. The ensemble-averaged shape of fractons and the superlocalization

Alexander *et al.*<sup>31,32</sup> have supposed that fractons on percolating networks are strongly localized in the form of

$$\phi_{fr} \sim \exp\{-[r/\Lambda(\omega)]^{d_\phi}\}, \quad (3.1)$$

where  $\Lambda(\omega)$  is the localization length depending on frequency, and  $r$  is a radial distance from the center. The exponent  $d_\phi$  indicates the strength of the localization. Excitations with  $d_\phi$  larger than unity are called "superlocalized" modes.<sup>17</sup> We have investigated the localized nature of fractons, paying much attention to the value of the exponent  $d_\phi$  and the localization length  $\Lambda(\omega)$  in Eq. (3.1). We have prepared *nine* 2D site-percolating networks at  $p_c$  formed on  $700 \times 700$  square lattices in order to average over as many fractons as possible. The maximum network size was  $N=171\,306$  and the minimum one  $N=76\,665$ . We excited 129 fracton modes in all, with eigenfrequencies close to  $\omega=0.01$  on nine percolating networks. The smoothly leveled mode patterns have been obtained by the procedure mentioned in the preceding section. The ensemble-averaged shape of the core of the fracton wave function was obtained by averaging over all these fractons. Figure 6 shows the ensemble-averaged shape as a function of a distance  $r$  from the center (open circles), and the log-log plot of  $r$  and  $-\ln(|\langle \phi_{fr} \rangle|)$  (filled circles). The straight line through filled circles is drawn from the least-squares fitting for the range  $r < 30$ , and the solid line through open circles represents the same line in a linear scale. The gradient of the straight line indicates the value of the geometrical exponent  $d_\phi$  of the ensemble-averaged fracton excitation. As a result, the geometrical exponent is obtained as  $d_\phi = 2.3 \pm 0.1$  and the localization length  $\Lambda(\omega=0.01) = 17.2$ . It should be remarked that this localization length  $\Lambda(\omega)$  is not the same with the size of the fracton which will be obtained from the inverse participation ratio or the moments of  $u^2$ .

In addition, we have calculated  $d_\phi$  and  $\Lambda(\omega)$  for four *different* eigenfrequencies;  $\omega=0.005, 0.006, 0.007,$  and  $0.008$ , excited on five percolating networks. The results are shown in Table I. It should be emphasized that the localization length  $\Lambda(\omega)$  clearly depends on frequency. Localization length is plotted as a function of frequency by a log-log scale in Fig. 7. The straight line drawn by the least-squares fitting indicates that  $\Lambda(\omega) \sim \omega^{-\lambda}$  with  $\lambda=0.71$ . The exponent  $\lambda$  is predicted to be  $\lambda = \tilde{d}/D$  by Alexander and Orbach.<sup>1</sup> Substituting the values  $\tilde{d} = \frac{4}{3}$  and  $D=1.89$  for 2D networks, the exponent  $\lambda$  should be 0.705. The fair agreement between the theory and our experiments suggests that we have treated surely *fracton* excitations in our ensemble. As seen in Table I, the geometrical exponent  $d_\phi$  takes the *same* value independent of frequencies within our numerical accuracy. This

value is larger than any theoretical predictions.<sup>17-19</sup> The origin of this discrepancy is discussed in Sec. IV.

## IV. CONCLUSIONS

We have performed computer experiments on the fracton dynamics of 2D and 3D percolating networks with large particle sizes ( $N > 10^5$ ). In the vicinity of the crossover between phonons and fractons, the DOS is smoothly connected [Fig. 3(b) and Fig. 4] and the results do not exhibit a notable steepness or a hump. These are in contrast with the effective-medium theory.<sup>25-27</sup> It should be noted that a self-consistent mode-coupling theory,<sup>33</sup> in which the correlation of networks is taken into account to some degree, does not predict a drastic change in the DOS in the crossover region. This tendency was also pointed out for the  $d$ -dimensional Sierpinski gasket by Southern and Douchant.<sup>34</sup> Our numerical results of the DOS correctly show that the integrated number of modes equals the degree of freedom. It seems that the absence of the hump in the vicinity of the crossover region implies the appearance of excess density of states in the phonon regime. Unfortunately, the numerical accuracy of the computed DOS did not allow to evaluate such an excess.

Though some experimental results for topologically disordered materials indicate the existence of a steepness or hump in the crossover region of the DOS,<sup>35-37</sup> the low-frequency inelastic light scattering experiments for superionic borate glass with fractal structure<sup>8</sup> show no steepness, nor do they show the hump in the crossover region. Furthermore, Brillouin scattering on a series of silica aerogels has revealed that the phonon-fracton crossover is characterized by smooth dispersion and loss curves.<sup>11</sup> It should be noted that systems used in experiments are not always regarded as percolating networks.<sup>38</sup>

The steepness observed in the above experiments could be considered to be attributable to the additional DOS relevant to the bond-bending force constant. There is a theoretical suggestion from a scaling argument that the DOS of a system with the appropriate relative strengths of bond-stretching and bond-bending elastic force constants can exhibit a hump in the vicinity of the crossover frequency.<sup>39</sup> This point has been discussed also by Buchenau *et al.*<sup>36</sup> from an experimental viewpoint. The existence of bond-bending force constant affects some fundamental properties of percolating networks such as the stability of structure<sup>40,41</sup> or the universality class.<sup>42,43</sup> This is an interesting problem itself.

The ensemble-averaged shape of the core of the fracton excitation has been treated on 2D percolating networks at percolation threshold  $p_c$ . When constructing the ensemble average of the core of fracton excitations, we have found  $\langle \phi_{fr} \rangle \sim \exp\{-[r/\Lambda(\omega)]^{d_\phi}\}$ , where  $\Lambda(\omega) \sim \omega^{-0.71}$  with the exponent in close agreement with the prediction of the fracton dispersion law for 2D percolating network ( $\Lambda(\omega) \sim \omega^{-\tilde{d}/D}$ ;  $\tilde{d}/D=0.705$ )<sup>1</sup>, and  $d_\phi = 2.3 \pm 0.1$ . The value of  $d_\phi$  is not consistent with any theoretical predictions derived for localized electronic impurity states.<sup>17-19</sup> These theories have argued for superlocalization on the basis of the known indices of the

chemical length, that is, they presumed that the localization is governed by the averaged distance  $\phi_{fr}(\langle r \rangle)$ , not the ensemble average of fracton functions themselves  $\langle \phi_{fr} \rangle$ . It appears that two problems, electronic impurity state and our problem, yield different values for  $d_\phi$ . For our vibrational problem, it would surely not be appropriate to discuss the exponent of  $\langle \phi_{fr}(r) \rangle$  in terms of the chemical length. This is because the individual realizations of  $\phi_{fr}$  have such an abrupt property that

$$\langle \phi_{fr} \rangle \neq \phi_{fr}(\langle r \rangle).$$

In addition, we should emphasize that the ensemble average of the *matrix element* may be different from the matrix element using the ensemble average of *fracton func-*

*tions*. For example, the Raman scattering intensity is proportional to the square of the elastic strain induced by fracton excitations.<sup>8-12</sup> For this case, the ensemble average of matrix elements for strained fractons should be taken into account. We hope that our numerical investigation presented in this article will provide new insight into the underlying properties of fractons.

#### ACKNOWLEDGMENTS

We thank R. Orbach for critical and useful discussion. The Hokkaido University Computing Center is acknowledged for the use of the supercomputer facilities. This work was supported in part by the Suhara Memorial Foundation and the Iwatani Naoji Science Foundation.

- <sup>1</sup>S. Alexander and R. Orbach, J. Phys. (Paris) Lett. **43**, L625 (1982).
- <sup>2</sup>R. Rammal and G. Toulouse, J. Phys. (Paris) Lett. **44**, L13 (1983).
- <sup>3</sup>R. Orbach, J. Stat. Phys. **36**, 735 (1984); R. Orbach, Science **231**, 814 (1986).
- <sup>4</sup>S. Alexander, Physica **140A**, 397 (1986).
- <sup>5</sup>S. Alexander, O. Entin-Wohlman, and R. Orbach, Phys. Rev. B **34**, 2726 (1986).
- <sup>6</sup>J. E. Graebner, B. Golding, and L. C. Allen, Phys. Rev. B **34**, 5696 (1986); **34**, 5788 (1986).
- <sup>7</sup>S. Alexander, O. Entin-Wohlman, and R. Orbach, J. Phys. (Paris) Lett. **46**, L549 (1985); Phys. Rev. B **32**, 6447 (1985); J. Phys. (Paris) Lett. **46**, L555 (1985); Phys. Rev. B **33**, 3935 (1985).
- <sup>8</sup>A. Fontana, F. Rocca, and M. P. Fontana, Phys. Rev. Lett. **58**, 503 (1987); Philos. Mag. B **56**, 251 (1987).
- <sup>9</sup>A. Boukenter, B. Champagnon, E. Duval, J. Dumas, J. F. Quinson, and J. Serughetti, Phys. Rev. Lett. **57**, 2391 (1986).
- <sup>10</sup>Y. Tsujimi, E. Courtens, J. Pelous, and R. Vacher, Phys. Rev. Lett. **60**, 2757 (1988).
- <sup>11</sup>E. Courtens, R. Vacher, J. Pelous, and T. Woignier, Europhys. Lett. **6**, 245 (1988).
- <sup>12</sup>E. Courtens, J. Pelous, J. Phalippou, R. Vacher, and T. Woignier, Phys. Rev. Lett. **58**, 128 (1987).
- <sup>13</sup>Y. J. Uemura and R. J. Birgeneau, Phys. Rev. Lett. **57**, 1947 (1987).
- <sup>14</sup>R. Orbach and K. W. Yu, J. Appl. Phys. **61**, 3689 (1987).
- <sup>15</sup>G. Deutscher, Y.-E. Lévy, and B. Souillard, Europhys. Lett. **4**, 577 (1987); G. Deutscher, Philos. Mag. B **56**, 725 (1987).
- <sup>16</sup>M. C. Maliepaard, J. H. Page, J. P. Harrison, and R. J. Stubbs, Phys. Rev. B **32**, 6261 (1985).
- <sup>17</sup>Y.-E. Lévy and B. Souillard, Europhys. Lett. **4**, 233 (1987).
- <sup>18</sup>A. B. Harris and A. Aharony, Europhys. Lett. **4**, 1355 (1987).
- <sup>19</sup>A. Aharony, O. Entin-Wohlman, and R. Orbach, Phys. Rev. Lett. **58**, 132 (1987).
- <sup>20</sup>M. L. Williams and H. J. Maris, Phys. Rev. B **31**, 4508 (1985).
- <sup>21</sup>K. Yakubo and T. Nakayama, Phys. Rev. B **36**, 8933 (1987).
- <sup>22</sup>K. Yakubo and T. Nakayama, Jpn. J. Appl. Phys. Suppl. **26**, 883 (1987).
- <sup>23</sup>K. Yakubo and T. Nakayama, in *Proceedings of the 2nd Yukawa International Seminar*, edited by H. Takayama (Springer-Verlag, Berlin, 1989), p. 217.
- <sup>24</sup>E. W. Montroll and R. B. Potts, Phys. Rev. **100**, 525 (1955).
- <sup>25</sup>O. Entin-Wohlman, S. Alexander, R. Orbach, and K. W. Yu, Phys. Rev. B **29**, 4588 (1984); G. Polatsek and O. Entin-Wohlman, *ibid.* **37**, 7726 (1988).
- <sup>26</sup>B. Derrida, R. Orbach, and K. W. Yu, Phys. Rev. B **29**, 6645 (1984).
- <sup>27</sup>P. F. Tua and S. J. Putterman, Phys. Rev. B **33**, 2855 (1986).
- <sup>28</sup>G. S. Grest and I. Webman, J. Phys. (Paris) Lett. **45**, L1155 (1984).
- <sup>29</sup>J. Chalupa, P. L. Leath, and G. R. Reich, J. Phys. C **12**, L31 (1979).
- <sup>30</sup>J. Adler and A. Aharony, J. Phys. A **21**, 1387 (1988).
- <sup>31</sup>O. Entin-Wohlman, S. Alexander, and R. Orbach, Phys. Rev. B **32**, 8007 (1985).
- <sup>32</sup>S. Alexander, O. Entin-Wohlman, and R. Orbach, Phys. Rev. B **34**, 2726 (1986).
- <sup>33</sup>R. F. Loring and S. Mukamel, Phys. Rev. B **34**, 6582 (1986).
- <sup>34</sup>B. W. Southern and A. R. Douchant, Phys. Rev. Lett. **55**, 966 (1985).
- <sup>35</sup>H. M. Rosenberg, Phys. Rev. Lett. **54**, 704 (1985).
- <sup>36</sup>U. Buchenau, M. Prager, N. Nuecker, A. J. Dianoux, N. Ahmad, and W. A. Phillips, Phys. Rev. B **34**, 5665 (1986).
- <sup>37</sup>A. J. Dianoux, J. N. Page, and H. M. Rosenberg, Phys. Rev. Lett. **58**, 886 (1987).
- <sup>38</sup>G. Deutscher, R. Maynard, and O. Parodi, Europhys. Lett. **6**, 49 (1988).
- <sup>39</sup>S. Feng, Phys. Rev. B **32**, 5793 (1985).
- <sup>40</sup>M. F. Thorpe and E. J. Garboczi, Phys. Rev. B **35**, 8579 (1987).
- <sup>41</sup>E. J. Garboczi, Phys. Rev. B **37**, 318 (1988).
- <sup>42</sup>Y. Kantor and I. Webman, Phys. Rev. Lett. **52**, 1891 (1984).
- <sup>43</sup>M. Sahimi, J. Phys. C **19**, L79 (1986).